Validation of a Multi-Purpose Depletion Chain for Burnup Calculation through TRIPOLI-4 Calculations and IFP Perturbation Method

P. Archier, S. Domanico, Jm. Palau, G. Truchet

VALIDATION OF A MULTI-PURPOSE DEPLETION CHAIN FOR BURNUP CALCULATIONS THROUGH TRIPOLI-4 CALCULATIONS AND IFP PERTURBATION METHOD

P. Archier, S. Domanico, J.-M. Palau, G. Truchet
CEA, DEN, DER, SPRC, Cadarache
Saint-Paul-Lez-Durance, F-13108, France
pascal.archier@cea.fr

ABSTRACT

The current standard depletion chain used by the CEA, called CEA-V5, was validated to treat only LWRs in 2008. This single depletion chain must correctly model the global loss of reactivity for both LWRs and Fast Reactors for future APOLLO3® work on Generation III and IV reactors such as EPR and ASTRID projects milestones. In order to verify the loss of reactivity of the standard CEA-V5 chain, a reference chain with 885 Fission Products (FPs) has been defined and used with the French Monte Carlo code TRIPOLI-4® and its depletion module for comparisons with the standard CEA-V5 chain containing 126 FPs. Three test cases are modeled, a UOX PWR cell, a MOX PWR cell and a MOX SFR cell, to validate the standard chain against the reference one. Results obtained from TRIPOLI-4® can then be used to calculate a loss of reactivity for each case to verify that the standard chain takes into account the majority (ideally 99.9%) of the anti-reactivity of the reference chain. In addition, this loss of reactivity has been decomposed by isotope to rank the FPs by importance using the Iterated Fission Probability (IFP) method recently implemented in TRIPOLI-4®.

Key Words: **Burnup calculation, depletion chain, validation**

1. INTRODUCTION

One of the main objectives of the new French core analysis code APOLLO3® [1, 2] is its ability to treat both thermal and fast reactors. The current standard depletion chain used by the CEA, called CEA-V5 (based on JEFF-3.1.1 Fission Yields and Decay Data library), was validated to treat LWRs in 2008 [3]. In order to implement a multi-spectrum depletion chain for the deterministic APOLLO3® code, this chain must be validated for both thermal and fast reactors. Effectively, this single chain must correctly model the global loss of reactivity for both LWRs and Fast Reactors (FRs) for future APOLLO3® work on Generation III and IV reactors such as EPR and ASTRID projects.

In order to verify the loss of reactivity (*i.e.* anti-reactivity) of the standard CEA-V5 chain, a reference chain with 885 fission products (FPs) is defined in the French Monte Carlo code TRIPOLI-4® (release 4.9 dev.) [4], coupled with a depletion module (MENDEL), to compare with the standard CEA-V5 chain containing 126 FPs. Three test cases are modeled in TRIPOLI-4®: a UOX PWR cell, a MOX PWR cell and a MOX SFR cell, each tested with both the standard chain and the reference chain. Results from TRIPOLI-4® can then be used to calculate a loss of reactivity for each case to verify that the standard chain takes into account the majority (ideally 99.9%) of the anti-reactivity of the reference chain.

In addition to analyzing the total amount of anti-reactivity, the loss of reactivity can be decomposed by isotope to rank the FPs by importance using the Iterated Fission Probability (IFP) method implemented in TRIPOLI-4®. This hierarchy can then verify that the correct and most relevant isotopes (absorbers) for both LWRs and FRs are present in the standard chain.

2. PRESENTATION OF VALIDATION CASES AND METHODS

2.1. Validation Cases

Three fuel cells were tested in the scope of this project: UOX PWR, MOX PWR and MOX SFR. Each cell type is modeled in TRIPOLI-4® as an infinitely long pin cell with cladding, a moderator/coolant, and reflections on all sides. The geometry, compositions, and enrichments of the PWR cells, whose section is pictured on the left in Figure 1, were based on the Mosteller benchmark [5]. To account for the non-linear radial distribution of fission rate and absorption in PWR cells, the fuel region is divided into four rings with thinner thicknesses closer to the moderator. The UOX cell was modeled at a 3.9 wt% U-235 enrichment while the MOX cell was modeled at 6 wt% PuO_2. The SFR test case, whose section is pictured on the right in Figure 1, was enriched to about 23 wt% PuO_2.

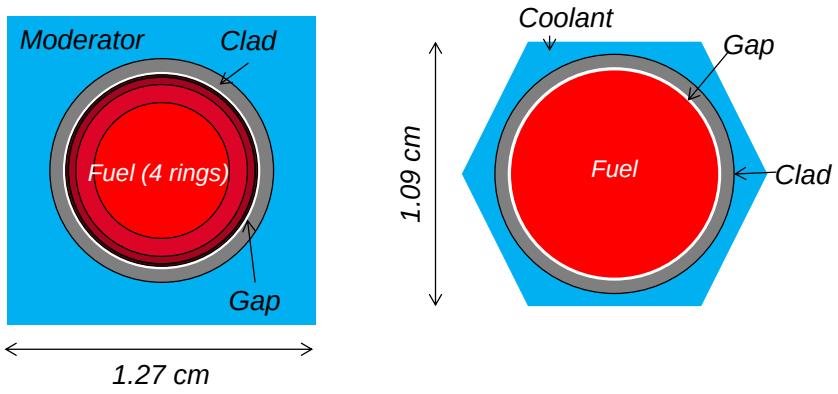

Figure 1. PWR cell geometry (left) and SFR cell geometry (right).

2.2. Depletion Chains

Each cell was tested twice, once with the standard CEA-V5 depletion chain, and once with the reference chain. The CEA-V5 chain in TRIPOLI-4® includes 126 FPs, 26 actinides, and 5 additional isotopes to correctly model the nuclear reactions in the chain. A total of 131 non-actinides influence the reactivity loss with the standard chain. The reference depletion chain includes 885 FPs and 26 actinides, with up to 863 non-actinides relevant for the anti-reactivity, depending on the test case. Nuclear data required by TRIPOLI-4® were processed from JEFF-3.1.1 library when available and TENDL-2014 library [6] when not.

With more absorbers present during depletion, it is expected that the reference chain would cause a greater loss of reactivity than the standard chain. The magnitude of this difference, however, is what determines the validity of the standard chain. If the standard chain accounts for the majority of the loss of reactivity, around 99.9%, for both the PWR cells and SFR cell, then the standard chain will be considered valid to be used in APOLLO3® for thermal and fast reactor applications.

2.3. Depletion Calculations

The final End-of-Cycle (EOC) concentrations for each cell with both depletion chains were calculated using the Monte Carlo code TRIPOLI-4® and its depletion module (MENDEL, also used in the APOLLO3® code). The PWR cell depletion calculations were carried out from 0 to 60 GWd/t with 46 burnup steps to be consistent with the previous TRIPOLI-4® study [7].

The SFR cell was depleted with 34 time steps from 0 to 14 400 days. The test cases with the standard chain were run with 100 batches of 100 particles and 256 independent simulations (100x100x256 histories). With the reference chain, the test cases were run with 100 batches of 100 particles and 64 independent simulations (100x100x64 histories). Those simulation parameters have been found from a convergence study presented in the next Section.

2.4. Loss of Reactivity and TRIPOLI-4® IFP

In order to calculate the k-effectives at the beginning and end of cycle for each cell[1], the test cases were run through TRIPOLI-4® without depletion module and with several thousands of particles (2.5×10^4) and batches (2×10^5) for maximum convergence. With the converged k-effective output from TRIPOLI-4®, an exact loss of reactivity between the beginning and end of cycle was calculated. The final loss of reactivity for each standard case was then compared to its reference case.

[1] With initial and final concentrations.

It is also possible to calculate a loss of reactivity using the IFP exact perturbation method recently implemented in TRIPOLI-4® by G. Truchet [8]. This TRIPOLI-4® IFP method is similar to the first order perturbation methods developed by Kiedrowski in the MCNP code [9]. This exact method uses both the adjoint and direct fluxes to calculate a loss of reactivity. Because the k-effective is dependent on the cross sections and concentrations of the isotopes, the loss of reactivity can then be decomposed by isotope [8]. This decomposition by isotope is particularly interesting to detail all the contributors, isotopes and reactions, of the global loss of reactivity for each depletion chain in order to eventually identify any relevant (or missing) isotopes.

3. RESULTS

3.1. TRIPOLI-4® Convergence Study

To show that the TRIPOLI-4® calculations were converged with respect to the final concentrations of the isotopes in the test cases, several isotopic concentrations for each cell with the standard chain were compared between two trials: the chosen 100x100x256 case and a sufficiently converged case (100x1000x256 and 200x1000x512 for the UOX PWR). The isotopes analyzed were chosen based on their known influence on the reactivity and the cycle. For instance some of the most effective absorbers, Xe-135 and Rh-103 for the UOX and MOX PWR cases, and Ru-101 and Tc-99 for the SFR case, were considered in the concentration convergence analysis. The concentrations of plutonium and uranium were also statistically analyzed and are presented in Table I for the UOX PWR case.

Table I. Comparison of End-Of-Cycle concentrations between the standard and reference concentration results for the UOX PWR case.

Isotopes	Concentration (C) 100x100x256	Concentration (C_{ref}) 200x1000x512	Difference in % $\lvert C - C_{\text{ref}}\rvert / C_{\text{ref}}$
Cs133	7.23992E-05	7.23823E-05	0.023348
Nd143	4.43573E-05	4.43532E-05	0.009244
Nd145	4.08761E-05	4.08749E-05	0.002936
Nd148	2.48172E-05	2.48182E-05	0.004029
Nd150	1.22543E-05	1.22544E-05	0.000000
Rh103	3.77022E-05	3.76919E-05	0.027327
Tc99	7.96418E-05	7.96424E-05	0.000753
Xe131	2.40035E-05	2.39954E-05	0.033756
Xe135	8.57640E-09	8.57737E-09	0.011309
U235	1.12381E-04	1.12308E-04	0.065000
U238	2.09608E-02	2.09609E-02	0.000477
Pu239	1.66682E-04	1.66676E-04	0.003600

The results gave no more than 0.065%, 0.074% and 0.53% maximum difference of concentration for the UOX PWR, MOX PWR and SFR cases respectively. Since the differences are neither near nor greater than 1%, the chosen simulation parameters, 100 batches of 100 particles, were concluded sufficient to calculate the final concentrations used for the loss of reactivity. In the case of the PWR cells, this is consistent with previous studies [7].

3.2. Exact Loss of Reactivity Calculations

Using the results from the TRIPOLI-4® k-effective values at the BOC and EOC, the losses of reactivity for each cell with both the standard and reference chains were calculated and compared. Table II shows the resulting loss of reactivity associated to its statistical uncertainty and fraction of loss of reactivity from the standard chain compared to the reference chain.

Initially, the goal was to verify that the standard chain accounts for 99.9% of the anti-reactivity of the reference chain. However, accounting for all the uncertainties associated with both TRIPOLI-4® and the nuclear cross sections, 99.6% and over was satisfactory to validate the standard chain with respect to the reference chain.

Table II. Comparison of loss of reactivity calculated with standard and reference chains.

	UOX PWR		MOX PWR		MOX SFR	
	Standard chain	Reference chain	Standard chain	Reference chain	Standard chain	Reference chain
$\Delta\rho_{\text{exact}}$ (pcm)	-42420	-42541	-25681	-25772	-11246	-11256
Stat. Unc. (pcm)	±24	±23	±31	±61	±22	±19
Standard/Reference	99.7%		99.6%		99.9%	

3.3. TRIPOLI-4® IFP Exact Perturbations

In addition to verifying the total anti-reactivity, the IFP exact perturbation method was used on each test case to check that no major isotopes were missing from the standard chain. The twenty first contributors for the three cases in terms of anti-reactivity are detailed in Table III.

As an initial check, the orders of the isotopes, classified from most important absorber to least important, were compared to previous published reports on anti-reactivity and FPs. Despite differences in enrichment and geometry, the PWR main contributors of the loss of reactivity remain in the same order as in the validation report of the CEA-V5 depletion chain [3]. The major absorbers are Xe-135, Rh-103, Nd-143, Cs-133, Xe-131 and Tc-99 in the PWR cases (see Table III and for more details, see also Table IV for the UOX PWR case and Table V for the MOX PWR case). It was noted, however,

that Xe-135m, which is not included in the standard chain, has an effect of -106 pcm (0.5% of total anti-reactivity due to FPs) and -53 pcm (0.4% of the total anti-reactivity due to FPs) in the PWR UOX and MOX cells respectively. The absence of Xe-135m in the standard chain, however, is accounted for in the effect of Xe-135, as Xe-135m quickly decays (about 15 minutes) to Xe-135. For the PWR perturbation calculations, the effect of diffusion on the anti-reactivity was neglected as it contributed to no more than 1.1% of the total anti-reactivity.

In the case of SFR cell, the use of the standard depletion chain leads roughly to the same isotope hierarchy presented in Reference [10] (despite enrichment and geometry differences). The major absorbers for the SFR cell are Ru-101, Rh-103, Tc-99 and Cs-133, as shown in Table III and more detailed in Table VI. The vast majority of the isotopes detailed in Reference [10] are found in the standard chain CEA-V5. Those, plus the additional isotopes in the chain, lead to the 99.9% of anti-reactivity. Overall, no significant differences between the standard and reference depletion chain were found that might require modifications.

Table III. List of 20st Fission Products (FPs) by order of contribution to anti-reactivity in a UOX PWR cell at 60 GWd/t, MOX PWR cell at 60 GWd/t and MOX SFR cell at 14 400 days.

UOX PWR			MOX PWR			MOX SFR (with diffusion)		
$\Delta\rho_{\text{pert}} = 42668 \pm 123$ pcm $\Delta\rho_{\text{exact}} = 42416 \pm 24$ pcm Agreement: 1.99σ $\Delta\rho_{\text{FP}} = 20031$ pcm			$\Delta\rho_{\text{pert}} = 25535 \pm 65$ pcm $\Delta\rho_{\text{exact}} = 25681 \pm 31$ pcm Agreement: 2.02σ $\Delta\rho_{\text{FP}} = 16672$ pcm			$\Delta\rho_{\text{pert}} = 11199 \pm 16$ pcm $\Delta\rho_{\text{exact}} = 11246 \pm 22$ pcm Agreement: 1.79σ $\Delta\rho_{\text{FP}} = 5261$ pcm		
	$\Delta\rho$ (pcm)	% of $\Delta\rho_{\text{FP}}$		$\Delta\rho$ (pcm)	% of $\Delta\rho_{\text{FP}}$		$\Delta\rho$ (pcm)	% of $\Delta\rho_{\text{FP}}$
Xe135	2424.63	12.105	Xe135	1944.54	11.663	Pd105	406.52	7.726
Rh103	2028.65	10.128	Rh103	1398.65	8.389	Ru101	394.64	7.500
Nd143	1652.65	8.251	Cs133	1072.87	6.435	Rh103	353.34	6.715
Cs133	1298.99	6.485	Sm149	990.09	5.938	Tc99	330.15	6.274
Xe131	1085.01	5.417	Nd143	954.49	5.725	Cs133	280.32	5.327
Tc99	988.54	4.935	Xe131	950.39	5.700	Pd107	270.87	5.148
Sm149	951.13	4.748	Tc99	805.28	4.830	Mo97	174.08	3.308
Eu153	740.94	3.699	Ag109	734.30	4.404	Sm149	169.59	3.223
Eu155	738.82	3.688	Sm152	668.82	4.011	Cs135	156.05	2.966
Sm152	732.23	3.656	Eu155	649.44	3.895	Ru102	135.91	2.583
Sm151	694.71	3.468	Eu153	641.55	3.848	Nd145	135.34	2.572
Eu154	689.68	3.443	Sm151	636.54	3.818	Mo95	134.02	2.547
Pm147	621.02	3.100	Eu154	600.94	3.604	Sm151	131.31	2.496
Nd145	590.31	2.947	Pm147	547.88	3.286	Nd143	118.13	2.245
Ag109	489.34	2.443	Nd145	391.50	2.348	Pm147	108.57	2.063
Ru101	435.39	2.174	Pd105	383.33	2.299	Ru104	103.71	1.971
Mo95	427.97	2.137	Ru101	382.70	2.295	Xe131	100.35	1.907
Pd105	319.48	1.595	Mo95	266.09	1.596	Mo100	97.90	1.861
Sm150	298.61	1.491	Pd108	241.34	1.448	Ag109	93.66	1.780
Pm148m	259.96	1.298	Pd107	226.37	1.358	Mo98	84.74	1.610

Table IV. List of all Fission Products (FPs) by order of contribution to anti-reactivity $\Delta\rho_{\mathrm{FP}}$ in a UOX PWR cell at 60 GWd/t.

Contribution in % of $\Delta\rho_{\mathrm{FP}}$ for UOX PWR cell	
$> 1\%$	Xe135, Rh103, Nd143, Cs133, Xe131, Tc99, Sm149, Eu153, Eu155, Sm152, Sm151, Eu154, Pm147, Nd145, Ag109, Ru101, Mo95, Pd105, Sm150, Pm148m, Cs134, Sm147
$0.1 - 1\%$	Pd108, Pr141, Pd107, Gd157, La139, Rh105, Kr83, Cs135, Mo97, Zr93, I129, Nd144, Gd156, Cd113, Mo98, Nd148, Eu156, Ru102, Pd104, I127, Mo100, Sm148, Ce141, Ru104, Cd110, Gd155, In115, Zr91
$0.01 - 0.1\%$	Zr96, Nd147, Nd146, Pm148, Xe133, Xe132, Cd111, Pd106, Pr143, Nd150, Ce142, Ba134, Pm149, Mo96, Br81, Ru100, Y89, Sm154, Dy162, Xe134, Ru103, Dy161, Ce140, Sm153, Gd158, Tb159, Nb95, Sr90, Gd154, Dy163, Dy164, Rb85, Cs137, Nd142, Se79, Ba138, Zr92, Ce144, Sb121, Ba137, Xe136, Rb87, Dy160, Sb123, Zr94, Ru106
$< 0.01\%$	Ho165, Kr84, Pm151, Te130, Zr95, Ag110m, He3, Cd114, Pd110, Te128, Tb160, Cd112, Sb125, Eu151, Xe130, Ba135, Kr85, Te125, Mo99, La140, Ba136, Kr86, Te127m, I131, Gd160, Er166, Eu157, Te129m, Cs136, Sr88, Dy165, Te131m, Ru105, I135, H3

Table V. List of all Fission Products (FPs) by order of contribution to anti-reactivity $\Delta\rho_{\mathrm{FP}}$ in a MOX PWR cell at 60 GWd/t.

Contribution in % of $\Delta\rho_{\mathrm{FP}}$ for MOX PWR cell	
$> 1\%$	Xe135, Rh103, Cs133, Sm149, Nd143, Xe131, Tc99, Ag109, Sm152, Eu155, Eu153, Sm151, Eu154, Pm147, Nd145, Pd105, Ru101, Mo95, Pd108, Pd107, Pm148m, Sm150, Sm147
$0.1 - 1\%$	Gd157, Cs135, Cs134, Pr141, La139, Mo97, Rh105, Cd113, Kr83, I129, Zr93, Gd156, Cd110, I127, Gd155, Mo98, Nd148, Ru104, In115, Ru102, Pd104, Mo100, Nd144, Sm148, Pd106, Cd111, Eu156, Ce141
$0.01 - 0.1\%$	Zr96, Dy162, Dy161, Nd150, Dy164, Nd147, Tb159, Dy163, Xe132, Zr91, Nd146, Xe133, Sm154, Pr143, Gd158, Pm148, Ba134, Gd154, Ce142, Ru103, Dy160, Br81, Xe134, Sm153, Sb121, Mo96, Pm149, Nb95, Ru100, Ce140, Cs137, Ho165, Sb123, Rb85, Ce144, Y89, Ba138, Ru106, Se79, Zr92, Ba137, Pd110, Sr90, Cd114, Eu151, Rb87
$< 0.01\%$	Xe136, Ag110m, Nd142, Cd112, He3, Zr94, Tb160, Sb125, Pm151, Te128, Zr95, Te130, Te125, Kr84, Ba135, BA136, Mo99, Xe130, La140, Kr85, Er166, Te127m, Gd160, I131, Kr86, Cs136, Te129m, Eu157, Sr88, Dy165, Te131m, Ru105, I135, H3

Table VI. List of all Fission Products (FPs) by order of contribution to anti-reactivity $\Delta\rho_{\mathrm{FP}}$ in a MOX SFR cell at 14 400 days.

Contribution in % of $\Delta\rho_{\mathrm{FP}}$ for MOX SFR cell (diffusion effects included)	
$> 1\%$	Pd105, Ru101, Rh103, Tc99, Cs133, Pd107, Mo97, Sm149, Cs135, Ru102, Nd145, Mo95, Sm151, Nd143, Pm147, Ru104, Xe131, Mo100, Ag109, Mo98, Pd106, Pr141, Sm147, Xe132, Eu153, Ce142, Xe134, Pd108, Zr93
$0.1 - 1\%$	La139, Nd146, Cs137, Sm152, I129, Nd144, Zr94, Nd148, Zr96, Xe136, Zr92, Zr91, Cd111, Ce140, Nd150, Eu154, I127, Ba138, Ru106, Eu155, Cs134, Sm150, Ce144, Pd104, Ru103, Ru100, Te130, Sm148, Gd157, Sr90, Y89, Pd110, Rb85, Gd156, Rb87, Kr83, Gd155, Sm154, Te128, Cd113, Cd112, Nb95
$0.01 - 0.1\%$	Cd110, Sr88, Kr86, Kr84, Ce141, Br81, Ba134, In115, Tb159, Ba136, Mo96, Zr95, Ba137, Pm148m, Gd158, Sb125, Eu151, Pr143, Cd114, Sb123, Nd147, Sb121, Te125, Se79, Xe130, Dy161, Gd154, Pm149, Kr85, Dy160, Mo99, Nd142, Ag110m
$< 0.01\%$	I131, Rh105, Xe133, Gd160, He3, Te127M, La140, Te129m, Dy162, Dy163, Pm148, Cs136, H3, Ba135, Xe135, Eu156, Ho165, Ru105, Dy164, Tb160, Pm151, Sm153, Te131m, Er166, I135, Eu157, Dy165

4. CONCLUSION

The standard depletion chain (CEA-V5), has been validated in this study for its use in APOLLO3®. Given that the standard chain in all three test cases amounts to at least 99.6% of the anti-reactivity of the reference chain, it can be concluded that the standard chain is valid for multi-purpose (fast and thermal) neutronic calculations and accounts for at least 99.5% of the loss of reactivity. In addition to verifying the use of the standard CEA-V5 chain for future use in APOLLO3®, this study confirms previous works [3, 10] on this topic.

Further work can still be done on the standard chain to increase the efficiency of APOLLO3® calculations. For instance, some isotopes at the end of the hierarchy could be removed to decrease calculation time. Other isotopes important for applications besides loss of reactivity might also be worth adding to the depletion chain so that the chain can serve for several different applications (burnable absorbers, decay heat, activation, fission gas cladding deformation…).

REFERENCES

[1] H. Golfier *et al.* "APOLLO3: a common project of CEA, AREVA and EDF for the development of a new deterministic multi-purpose code for core physics analysis." In: *International Conference on Mathematics, Computational Methods and Reactor Physics (M&C 2009)*. American Nuclear Society (ANS). Saratoga Springs, New York, USA, May 3 - 7 (2009).

[2] D. Schneider *et al.* "APOLLO3®: CEA/DEN Deterministic Multi-Purpose Code for Reactor Physics Analysis." In: *This PHYSOR 2016 Conference*. Americal Nuclear Society. Sun Valley, Idaho, USA, May 1 - 5 (2016).

[3] S. Mengelle, D. Bernard, and J.-F. Vidal. *Détermination et éléments de validation de la chaîne d'évolution à 162 noyaux et 126 PF pour les bibliothèques CEA2005 V4.1. Technical Report DM2S/SERMA/LLPR/RT08-4397/A*, Commissariat à l'Énergie Atomique, Saclay, France (2008).

[4] E. Brun *et al.* "TRIPOLI-4®, CEA, EDF and AREVA reference Monte Carlo code." *Annals of Nuclear Energy*, **82**: pp. 151–160. Joint International Conference on Supercomputing in Nuclear Applications and Monte Carlo 2013, SNA + MC 2013. Pluri- and Trans-disciplinarity, Towards New Modeling and Numerical Simulation Paradigms (2015).

[5] R. Mosteller. "The Doppler-Defect Benchmark: Overview and Summary of Results." In: *Mathematics & Computation and Supercomputing in Nuclear Applications (M& C + SNA 2007)*. American Nuclear Society. Montery, California, USA, April 15 - 19 (2007).

[6] A. Koning and D. Rochman. "Modern Nuclear Data Evaluation with the TALYS Code System." *Nuclear Data Sheets*, **113(12)**: pp. 2841–2934. Special Issue on Nuclear Reaction Data (2012).

[7] E. Brun, E. Dumonteil, and F. Malvagi. "Systematic Uncertainty due to Statistics in Monte Carlo Burnup codes: Application to a Simple Benchmark with TRIPOLI-4-D." *Progress in Nuclear Science and Technology*, **2**: pp. 879–885 (2011).

[8] G. Truchet *et al.* "Sodium void reactivity effect analysis using the newly developed exact perturbation theory in Monte-Carlo code TRIPOLI-4." In: *PHYSOR 2014 - The Role of Reactor Physics toward a Sustainable Future*. American Nuclear Society. Kyoto, Japan, September 28 - October 3 (2014).

[9] B. C. Kiedrowski. *Theory, Interface, Verification, Validation, and Performance of the Adjoint-Weighted Point Reactor Kinetics Parameter Calculations in MCNP. Technical Report LA-UR-10-01700*, Los Alamos National Laboratory (2006).

[10] J. Tommasi. *Création de pseudo-produits de fission pour ERANOS (bibiliothèques JEFF-3.1). Technical Report DER/SPRC/LEPh/NT06-201*, Commissariat à l'Énergie Atomique, Cadarache, France (2006).